DESIGN AND CONSTRUCTION OF AN ARMILLARY SPHERE FOR ASTRONOMY TEACHING

Preprint · May 2023

DOI: 10.13140/RG.2.2.36568.16641/1

Ademir Xavier
Brazilian Space Agency

Design and construction of an armillary sphere for astronomy teaching

Ademir Xavier Jr.
Brazilian Space Agency,
CEP 70610200, Brasília - DF*
(Dated: May 5, 2023)

An ancient astronomical instrument and its use in astronomy are briefly reviewed. A detailed description and construction of an armillary sphere of cardboard and paper are presented. Then, it is used to introduce basic notions in positional astronomy, especially the concepts of time (mean solar, true, sidereal), the influence of the observer's position in the determination of the azimuth angles of sunrise, sunset, and meridian passage of planets whose longitude is set along the ecliptic. One concludes that the model acts as a small, easy-to-use mechanical calculator that can effectively teach astronomy concepts.

Keywords: armillary sphere, spherical astrolabe, spherical astronomy, astronomy teaching.

I. INTRODUCTION

The invention of the telescope in the early 17th century (King 2003) impacted astronomy just as the internet and fast electronic processors revolutionized the way to do science in the late 20th century. The telescope provided accurate values of celestial bodies' position and time as a result of their optical magnification. However, after the telescope, ancient astronomical instruments were almost completely neglected in favor of the new invention. Similarly, popular electronic devices were totally forgotten after electronic processors were incorporated into cell phones (fax machines, copiers, recorders, etc).

One of these forgotten but venerable instruments is the armillary sphere, also called "spherical astrolabe" (Figure 1). In the West, Greek references are known since the 3rd century BC at least for the so-called "demonstrational version" (Mosley 1999). Armillaries are considered the most important astronomical instruments in ancient China since the 4th century BC (Sun 2005, Lee et al. 2010). They were relevant devices in Islamic and Indian astronomy (Khan 2007, Lu 2015). In Europe, the apex of their development and manufacture took place in the 10th century, culminating with Tycho Brahe's observational armillary at the end of the 16th century (Wesley 1978).

Like astrolabes, sextants, and quadrants (Egler 2006), armillary spheres were regarded as "mathematical instruments" in the past (Bennett 2011) because they worked as mechanical computers for quick position and ephemeris determination (Evans 1998). Nowadays, armillary spheres have become stylish items for rooms and gardens and can be considered symbols of knowledge (Aterini 2022). However, modern astronomy teaching can benefit from their usage and, even more, from classes in which students are taught to build and operate them (Gangui et al 2014, Zhang et al 2014).

The objective of this work is to detail the design and construction of an armillary sphere and to describe the demonstrations in positional astronomy that are possible through it. We begin our work with a brief discussion of minimum layout (Section II). Design and implementation instructions are then given (Section III). Materials and tools are described in Section IV. The assembly of the armillary sphere is covered in Section V. In the final part, a brief discussion of possible demonstrations (Section VI) and accuracy estimates (Section VII) is presented. Section VIII presents the conclusions of the work.

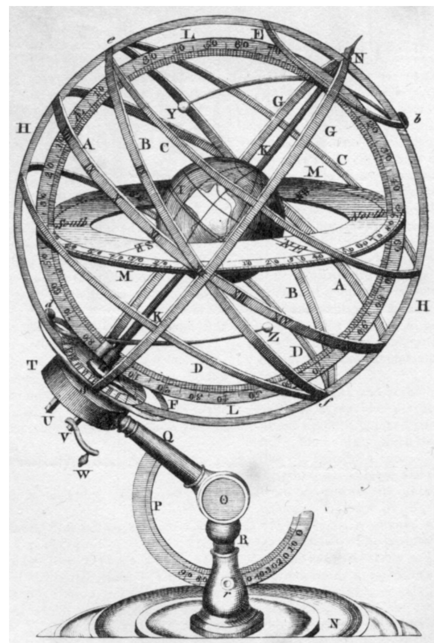

FIG. 1. Diagram of an armillary sphere, 1771. Source: Wikipedia. From Society of Gentleman in Scotland, Encyclopedia Britannica, Vol. II, p. 681.

II. MINIMUM LAYOUT

Armillary spheres are of two types: "demonstrational" and "observational" (Mosley 1999). The observational

* email: xavnet2@gmail.com

type allows the determination of the astronomical coordinates of objects and their rise and set times. For this aim, time is counted (with the help of a clock) by a special marker on the sphere. The minimum design is composed of a set of 5 "great" circles representing (following the letters in Figure 1): (i) the observer horizon (or horizon circle, "M"), (ii) the local observer meridian (the meridian circle, "H"), (iii) the celestial equator ("A"), (iv) the ecliptic (or the ecliptic circle, "B"), (v) an equinoctial or solstitial colure ("G") for supporting the celestial axis ("K") as well as the ecliptic and equator circles (inner moving circles). Other circles are added to represent the tropic of Cancer ("C"), Capricorn ("D"), and the arctic and antarctic circles ("E" and "F", respectively). The inclination of the inner circles, which determines the position of the ecliptic and celestial equator, depends on the observer's latitude to be reproduced.

The armillary sphere is a sky model for the observer's topocentric position (*locus observationis*). As a legacy of geocentrism, the inner circles - on which the sun, moon, and planets are fixed - rotate about this place. However, any other object in the sky can be emulated by an appropriate marker attached to projections from the inner circles ("Y" in Figure 1). Each circle is engraved with ticks for angle reading: azimuth and elevation on the outer fixed circles; right ascension and declination on the celestial equator ring and colures, respectively; ecliptic longitude on the ecliptic circle.

Another circle can be installed parallel to the celestial equator to mark the time as an hour angle. This provides a time scale using predetermined objects or references as indicators: for the sun it is the observer's local time and for the vernal point the sidereal time. Depending on the accuracy of the sphere, the hour angle of the true sun position must be corrected by the equation of time (ET, Hugues et al 1989) in order to obtain the observer's civil time accurately (see Section VII). Many concepts in spherical astronomy are therefore involved in the understanding and manipulation of an armillary sphere.

III. DESIGN

The proposed design follows very closely the minimum arrangement described in the previous section. Using Figure 2 as a reference, the celestial equator circle (*Cq*) was initially planned to be orthogonal to the (solstitial) colure. However, a horizontal strap (parallel to the celestial axis) attached to the colure was chosen to represent this circle. The ecliptic (*Ce*) makes an angle of 23.5° with *Cq*, and the intersection of these two circles are the vernal (♈) and autumn points. The observer's latitude, φ, can be changed by a pair of adjustable bearings (*Fp*) holding the celestial axis (*Cx*). To read hour angles, an adjustable circle attached to the meridian (*Ct*) was implemented. However, to test the model a fixed latitude of 15° was chosen as a reference to the author's place in Brasília/DF (≈15.8° South).

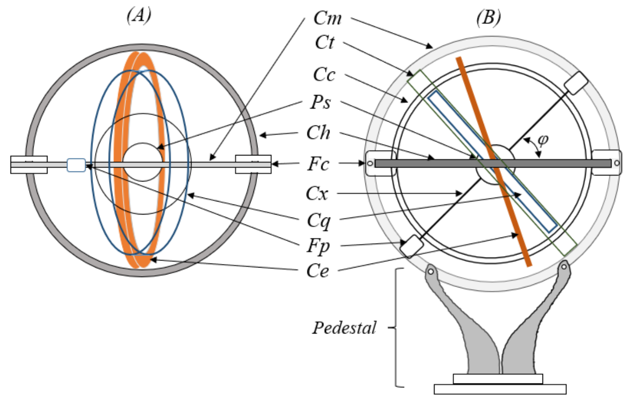

FIG. 2. (A) top and (B) side drawings of the proposed armillary sphere. Legends: *Cc*: colure, *Ce*: ecliptic circle, *Ch*: horizon circle, *Cm*: meridian circle, *Cq*: equatorial circle, *Ct*: hour angle grid, *Cx*: celestial axis, *Fc*: fixing clip, *Fp*: celestial pole pivot, *Ps*: Styrofoam sphere (Earth). φ is the observer's latitude angle. Source: author.

Circle	Ext⌀ [mm]	Max. width [mm]
Meridian (*Cm*)	361	25
Horizon (*Ch*)	310	24.5
Ecliptic (*Ce*)	259	16
Colure (*Cc*)	226	15.5
Equator (*Cq*)	226	20
Hour-angles (*Ct*)	310	20
Earth (*Ps*)	50	

TABLE I. External diameter (Ext. ⌀) and maximum width of the circles in Figure 2 in millimeters. Since the celestial equator (*Cq*) is the innermost circle, its diameter is not fixed. Source: author.

Figure 2 shows views of the proposed design where the values are in millimeters for each element dimension as shown in Table I. The diameter D_i of a given circle circumscribed by another one with diameter D_{i+1} and width w_{i+1} is $D_{i+1} - 2w_{i+1}$. One or two millimeters are subtracted from this last value to facilitate the assembly.

The clamps used to hold the outer circles and pedestal are also made of the same materials following the instructions of Fig. 12(A) and Section IV. Pole bearings are built on the set of smaller clamps attached to the meridian circle as shown in Fig. 12(B).

The measures of the pedestal structure are given in Fig. 13. A set of 4 "feet" (Fig. 13B) hugs the meridian ring (*Cm*). This set is fastened to the meridian circle by means of 2 screws (and nuts). The feet are glued to the base (Fig. 13C) using two cardboard brackets (Fig. 13A).

IV. MATERIALS AND TOOLS

Armillary spheres were made of metallic materials such as iron and brass (Paselk 2015) besides wood. Recently, models using MDF (medium-density fiberboard) have also been commercialized. Cardboard, styrofoam, paper, metal screws, and wooden sticks were used in the model proposed here. These materials have the advantage of being easy for students to work with, enabling them to use leftovers from other projects. Disadvantages include the need for careful handling and keeping the materials and the work result away from water. Having selected these materials, the tools required for the model assembly are a ruler, paper, glue, a pencil, and a compass.

The model structure (outer, inner circles, and pedestal) was made of a piece of thick cardboard (B-flute double-wall, 1/4" or 6.35 mm) with 400 X 400 mm^2 size. The sheet is easily cut using a utility knife. The celestial axis is made of a single wood stick (296 mm long) perforating the colure (Cc). The axis also penetrates a Styrofoam sphere representing the Earth (Fig. 4a). The model was covered with paper and EVA (ethyl vinyl acetate) foam sheets, although the latter is not required. For assembly, PVA (polyvinyl acetate) glue was used.

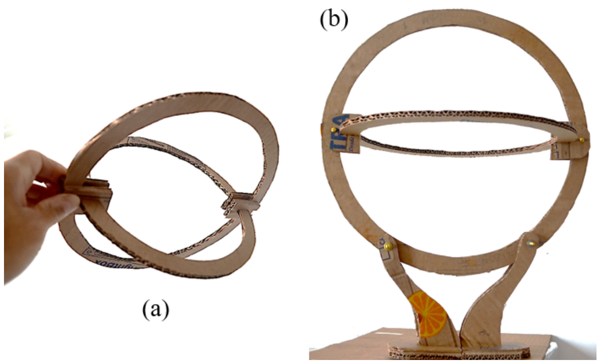

FIG. 3. Assembly of the unfinished inner and outer circles: (a) Cc and Ce and (b) Ch and Cm. Double-wall cardboard was used following the measures of Table I.

A compass was used to mark the angles on the circles. For a given angle θ, the mark should be located at $s = r\theta$ from the origin for a circle of radius r. For a circle of diameter D, the chord length C for angle θ is $D\sin(\theta/2)$. The orientation of the graduated circles depends on the observer's position. To represent the movement of the sky in another hemisphere, the inner circles must be flipped (corresponding to reversing the sign of the latitude angle), a fact the students soon realize while building the sphere.

V. ASSEMBLY

The building process is outlined by the following steps: i) Cutting the inner and outer circles; ii) pre-assembly of the circles (Fig. 3b); iii) semi-finishing of each circle; iv) Cutting and assembling of the base; v) Finishing the circles and base (EVA covering), and vi) Preparing the grids of the main circles.

Construction begins by cutting out the circles (Fig. 3a) from the cardboard sheet. Then they are coated with (sulfite) paper as a pre-finish (Fig. 4). Thick carton sheets were used to make Cq and Ct as transversal circles or cylindrical sections. The hour angle (Ct) is attached to Ch by wood sticks along the west-east axis (Fig. 6). In this way, Ct can be adjusted to give the hour angle for different latitudes resulting from distinct positions of the pole pins. To facilitate the alignment of the meridian circle (Cm), it is recommended to pen preliminary azimuth marks on top of Ch. These indications will be replaced by the final grids after coating the whole structure with EVA sheets.

The outer circles are fixed by a set of clamps as shown in Fig. 4a using two metallic screws. They are attached to the base supports by a pair of screws and nuts. The inner circles Ce and Cq are glued and fixed to each other using toothpicks (Fig. 6). Sticking the parts with glue requires minimal drying time to avoid misalignment of the structure. After assembly, the final EVA coating applied changed the outer diameters of the circles by nearly 2 mm.

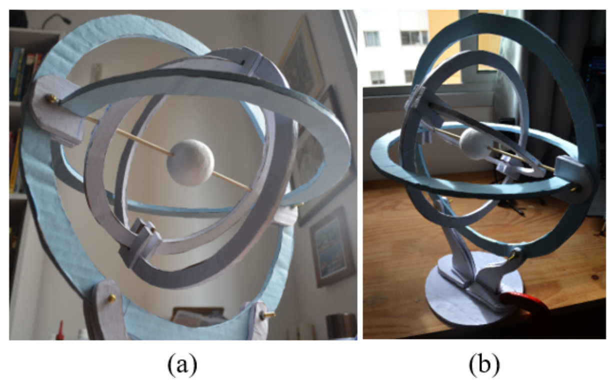

FIG. 4. Prefinished model. In (a) the celestial pole clamps (Fp) are not set up as in (b). The colure Cc is perpendicular to the plane of the celestial equation Cq. The design was later changed to accommodate Cq as a cylindrical section (parallel to the axis) and Ce. To this first assembly, Ct was not added yet.

The angle grids are either written on paper (or thin cardboard) or printed. In the present case, they were drawn directly on each paper circle with a pencil and ballpoint pen. Six angle graduations were made for the following intervals and steps (using as references Fig. 8 and 9): (i) Cm, elevation angle $A = \{0°, 90°\}$, $\delta A = 2°$; (ii) Ch, azimuth angle $A_z = \{0°, 360°\}$, $\delta A_z = 2°$; (iii) Ce, ecliptic longitude $\lambda = \{0°, 360°\}$, $\delta\lambda = 1°$, Ce; sun's position in time $\lambda_\odot = \{1, 12\}$ month, $\delta\lambda_\odot = 1$ week; (iv) Cc, declination $\delta = \{-90°, 90°\}$, $\delta\lambda = 2°$; (v) Cq, right ascension $RA = \{0, 24h\}$, $\delta RA = 10$'; and (vi) Ct, hour angle $t = \{0, 24h\}$, $\delta t = 10$'. Since an effective diameter of 362 mm was used for Cm, angles of 10° in elevation are separated by 31.5 mm. For all circles (except Ce), an angular step of 2° was chosen to account for the model uncertainty (see Section VII). For Ct, the minimum increment in t is 10 minutes which corresponds to 2.5° or 5.4 mm.

Gluing the *Ce* grid took place only after the inner circles were fully assembled. Two grids were represented on it: the (geocentric) longitude angle λ, and a time (month) scale $\lambda_\odot$ measured from Υ in months and divided into steps of weeks corresponding to the position of the sun throughout the year. It is important to consider that these grids are not fixed. The precession of the Earth changes the position of Υ. Therefore, on improved models, such grids should be adjusted separately. When used several years apart, typical errors of cardboard models (Section VII) do not justify separating the two circles. Finer solar positions along *Ce* are possible using the longitude ticks which were drawn at 1° steps.

FIG. 5. Finished bearings of the celestial axis (*Fp*). The measures of each piece follow the diagrams of Fig. 12.

FIG. 6. Fastening *Ch* to *Ch* using a piece of wood stick as a "rivet" at the West cardinal point. The hour angle circle (*Ch*) can be adjusted to the observer's latitude.

As for the orientation of *Cq* and *Ce* angle scales, the right-hand rule (RHR) requires angles to increase counterclockwise. However, when viewed from the south, longitude and right ascension increase clockwise with the thumb pointing north. Thus north oriented right ascension angles are written clockwise on *Cq* as seem from the south. The directions of these angles from the vernal point are summarized in Fig. 7.

The same RHR can be applied to get the orientation of the azimuth grid. For southern observers, azimuth increase from north to east by pointing the thumb toward the nadir. On the other hand, the hour angle *Ct* increases counterclockwise from east to west when viewed from the south by applying RHR with the thumb pointing south. This is because the motion of the Earth follows the RHR (with the thumb pointing north).

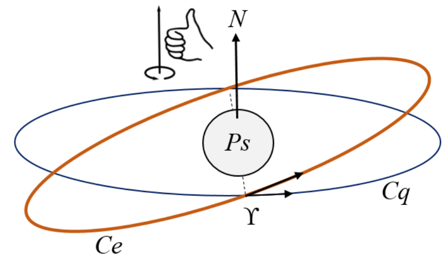

FIG. 7. The arrows indicate how angles on *Cq* and *Ce* increase from the vernal point (Υ) using the RHR pointing north.

Images of the finished model are seen in Fig. 9 and 10.

VI. DEMONSTRATIONS

Once the model is assembled, its manipulation is very simple and can be summarized by demonstrations of the following concepts:

1. The observer topocentric system. With the inner circles removed, the device embodies the observer's location (Fig. 8) and its relation to the topocentric system represented by the external circles. An observer is at the surface of the Earth (*Ps*) and sees the horizon (*Ch*) and the (local) meridian (*Cm*) as great orthogonal circles of the celestial sphere. Azimuth (*Az*) is measured from north to east, so that the east and west cardinal points are located at 90° and 180° from north respectively. The elevation or altitude angle (*A*) of an object is measured from the horizon to the zenith (*Z*).

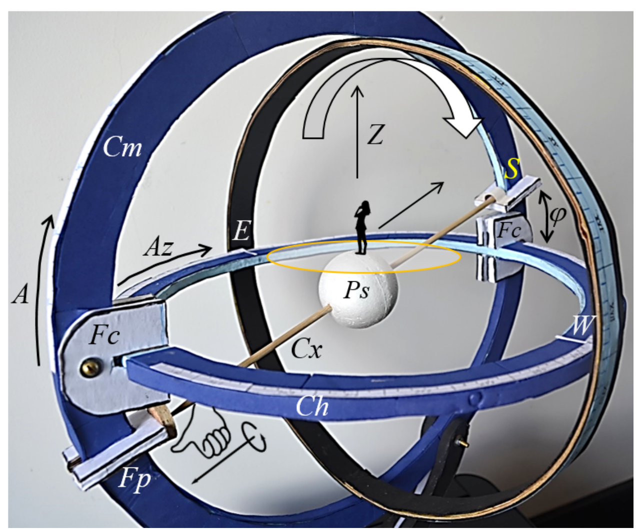

FIG. 8. Demonstration of the observer's topocentric coordinate system and other concepts using the device with the inner circles removed.

For an observer at latitude φ in the southern hemisphere, the *south* celestial pole is elevated above the horizon by an angle φ. Objects in the sky apparently move from E to W as if the celestial axis (Cx) rotated about the celestial pole (Fp) following the RHR, and the thumb pointing south. In fact, the Earth rotates eastward in accordance with the same role but with the thumb pointing north as shown in Figure 8. The apparent rotation of the celestial sphere is therefore a kinematic effect caused by the rotation of the Earth itself, and the celestial axis is an extension of the Earth's axis of rotation.

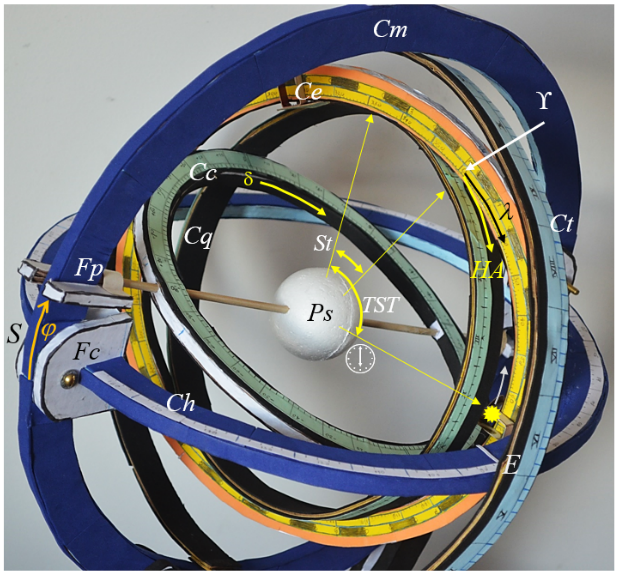

FIG. 9. Identifying the inner circles and the position of the origin of the coordinate system.

2. Ecliptic and celestial equator. With inner circles positioned as shown in Fig. 9, the device illustrates the motion of the celestial sphere represented by the celestial equator (Cq) and the ecliptic (Ce) in relation to the local coordinate system. A fundamental origin of this system is the vernal point (Υ) from which the hour-angle (HA) and ecliptic longitude (λ) are measured. Both angles increase eastwards in accordance with the RHR and thumb pointing north.

3. Introducing time. The movement of the inner sphere determines the passage of time, with the sun being the most important dial. True sun local time (relative to Cm, TST in Fig. 9) is obtained by reading the sun's position along Ct. Similarly, the (local) sidereal time St is the hour angle of Υ given by Ct. The first time is a convenient tool for human affairs, while the latter is a useful way to calculate the rise and set times of other objects represented in the inner circles.

To obtain the local time of an event simulated by the armillary sphere, a pre-computed time correction (TC) value must be applied to all solar hour angles. The Ct angle is 6:00 for the rising sun and 18:00 for the setting sun as read on the Ct grid for all days of the year. However, for the observer's longitude (48.01°W, LSTM=-45°) on March 21 for example, there is a 19-minute delay as the sum of two terms: a (fixed) time difference between the observer's longitude and the local standard time meridian (LSTM) and the (changing) ET (Hugues et al 1989). The first factor is LSTM = -12.04 minutes ($= 4 \times (48.01 - 45)$). Therefore TC = -12.04 min + ET(t) with ET(t) (=-7.22 min on March 21) providing the link with the Earth's orbital motion. Values of ET as a function of the sun's longitude can be written on Ce thus providing a quick way to find the local civil time of an event.

4. The sundial. As explained in (Evans 1998), the sphere can be used as a sundial if Cm is aligned with the north-south line and Cx is adjusted to the observer latitude. Under a sun-shining sky, the shadow of Cx on Ct gives the true sun local time.

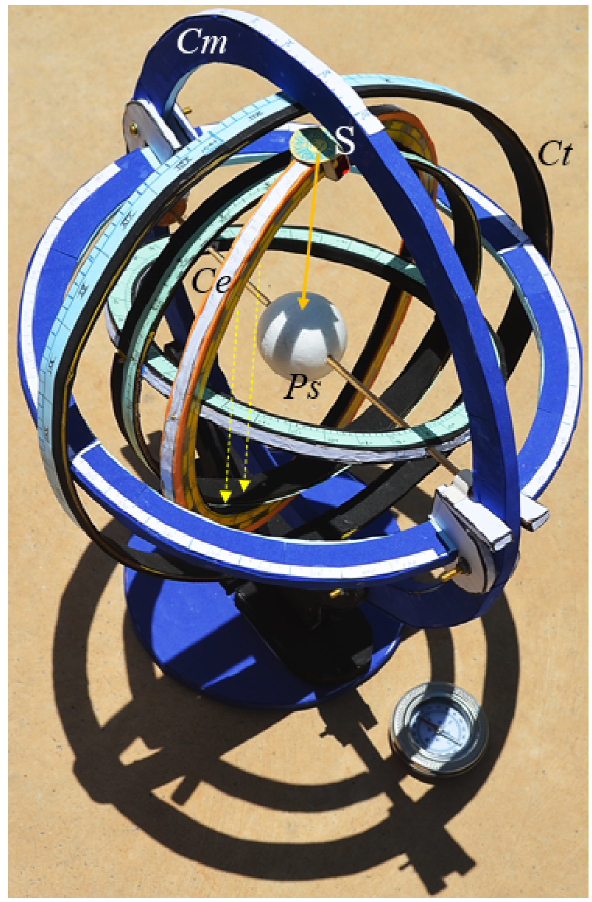

FIG. 10. The armillary sphere as a sundial. The sun S casts a shadow on Ps on March 4 2023 at 12:23 local civil time corresponding to 12:00 of the local true solar time at the observer coordinate (longitude 48.01° W). A magnetic compass was used to find the meridian line. The shadow of Ce is also exactly on Ce which occurs for the sun's longitude for the date.

Figure 10 shows the shadow of the sun marker on Ps on March 4, 2023 at 12:23 PM civil time, after the armillary sphere model is aligned with the meridian using a magnetic compass. The magnetic declination of the observer's location (approximately 22° W) was used (Alken et al 2021). On this day, ET is about -11.47 minutes, so the Sun is at the meridian line (Az=0, Ct=12:00) and the corresponding modified civil time is Ct - TC = 12:23.5 PM. The altitude of the sun measured by the sphere was about 80°, but a more accurate value is 79.76° (as given by exact ephemeris calculation, see next section). *Ce* and his shadow lined up on this date (Evans 1998) which is only possible if the sun marker is at longitude 345.78°, or 180° before or after this value (September 8th).

VII. ESTIMATING THE ACCURACY

Questions remain about the accuracy of the proposed model in determining the ephemerides of events such as rising, meridian passages, and setting times. Perhaps the only armillary sphere whose accuracy was recently determined was Tycho Brahe's iconic sphere (Wesley 1978). Despite its "demonstrational" character, the device can operate in the "observational" mode by using it to get ephemeris estimates. It is quite intuitive to expect low accuracy given the materials, pointing difficulties, and techniques used in its construction. To estimate the accuracy, one can define a measurement error as the observed difference between the reading and the actual coordinate or time of a particular event.

A simple way to get reference values is to use planetarium software such as Stellarium (Zotti et al 2021 and the online version https://stellarium-web.org), which gives the azimuth and elevation coordinates for celestial bodies in the sky. On the other hand, one can manually compute the object ephemeris for a given date and observer coordinates. When retrieving ephemerides for rising and setting events, it is recommended to use the software in "removed atmosphere mode", as atmospheric refraction changes the position of objects close to the horizon in about 35' (Comstock 1910).

TABLE II. Azimuth angles of Mars for $A = 0$ as given by Stellarium A_z(S) and the model A_z(AS) for the indicated dates (month/day/year format). The azimuth errors were rounded and are given by ΔA_z. LT(S) is the predicted local time according to Stellarium and the model respectively. ΔLT is the error in minutes. If $A_z < 180°$ the planet is rising, otherwise it is setting.

Date	A_z(S)	A_z(AS)	ΔA_z	LT(S) h	LT(AS) h	ΔLT
12/6/22	63.95°	60°	4°	18.67	18.38	16.9
3/4/23	296.52°	292°	4.5°	0.18	0.23	-2.8
10/15/23	257.35°	258°	-0.6°	18.83	18.8	2.1
9/7/24	65.6°	66°	-0.4°	1.65	1.83	-10.9
11/18/25	246.5°	248°	-1.5°	19.33	19.29	2.8

An alignment test involves finding the predicted azimuth of the rising $A_z^{(r)}$ and setting $A_z^{(s)}$ sun at a given date as well as its altitude angle $A^{(mp)}$ at the meridian passage on the same day. An easy date is the origin of the ecliptic (the vernal point) which happens between March 20 and 21 taking 2023 as the year. In principle, the azimuths are 90° and 270° for the rising and setting sun at the vernal point, respectively. In 2023 for the observer coordinates (15.836° S, 48.011° W), the sun rises at 6:18 and sets at 18:18 on March 21 2023 with $A_z^{(r)} =$ 89°55' and $A_z^{(s)} =$ 270°24', respectively. In fact, for example, $A_z^{(r)}$ is slightly less than 90° because the sun is past the vernal point when it rises at the observer place. The sun's elevation at the meridian passage on March 21 reads $A^{(mp)}$=74° against 73°55' as given by Stellarium.

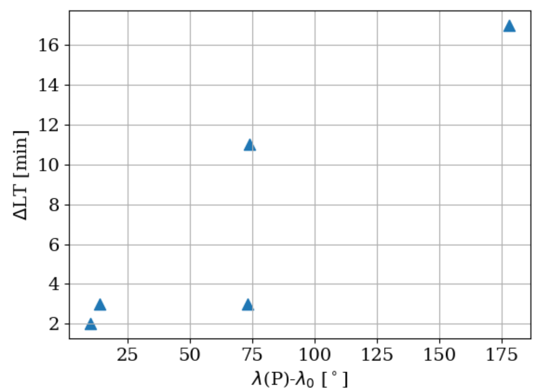

FIG. 11. Scatter plot showing the distribution of predicted event times errors ΔLT in minutes for the data in Table II as a function of the difference between the planet's longitude $\lambda(P)$ and the sun's λ_0 in degrees.

An assessment of the overall accuracy of the armillary sphere model can be seen in Table II. For distinct dates, rising or setting azimuths of Mars and their respective times were found using Stellarium (S) for the observer coordinates. Then, the markers for the sun and Mars were set to the ecliptic longitudes using the armillary sphere model (AS) disregarding the planet's ecliptic declination ($|\delta_\epsilon| \lesssim 2°$) and the corresponding azimuth and Ct were read. For each date, the corrected local times were retrieved by applying TC and ET as described in the previous section. The errors in the event time are $\Delta LT = LT(S) - LS(AS)$ in minutes, while the error in azimuth is $\Delta A_z = A_z(S) - A_z(AS)$ in degrees.

An error spread is observed at a maximum of 4.5 degrees in azimuth and 17 minutes in LT. However, based on other rising/setting dates (not shown in Table II), typical errors are ±2° in azimuth and ±10 minutes in ΔLT. The error appears to increase with the longitude difference between the planet $\lambda(P)$ and the Sun λ_0, which is most noticeable in LT. Figure 11 shows this relationship for the points in Table II. These values correspond to the intuitively expected accuracy of the model given the materials and techniques used in its construction.

VIII. FINAL DISCUSSION

As mentioned in (Evans 1998), the armillary sphere was an instrument used by Ptolemy to determine the longitude of celestial bodies. This was one of his methods based on "mathematical instruments", in addition to other more complicated ones dispensing such tools and using the positions of the moon and the sun. Assembling, aligning, and using the armillary sphere in this way is equivalent to reproducing an astronomy teaching method used by ancient Greek students, dating back at least 2000 years. The assembly process is an educational and recommended activity, complemented by domain-specific tasks in positional astronomy and ephemeris calculations. The educational value is greater when students learn to build the model rather than just work with it.

In this study, it was shown that it is also possible to assemble, calibrate and use an armillary sphere model using very simple materials and tools. However, some care must be taken to prepare and glue its components - giving the student the notion of "fabrication quality". Care is necessary to avoid misalignment among the various circles, but reducing such errors beyond a minimum is impossible given the size and type of materials used. The number and size of the rings can be changed without affecting the final result. However, larger structures are more difficult to handle and use, and adding more weight may require stiffer materials making the assembly task less economical and more time-consuming. By contrast, errors are reduced by using harder materials and larger circle sizes.

The assembled sphere can be used in two ways: i) as a model demonstrating the movement of the sky, celestial reference systems, and the position of the observer; ii) as a calculation tool in the "observational", despite the accuracy observed with the model. In this case, it is possible to "mechanically" calculate approximate values for the rising and setting azimuth angles of celestial objects represented on it. The accuracy was assessed in terms of rising/setting azimuth errors and times. Typical errors of $\pm 2^\circ$ in azimuth and 10 minutes in time were observed.

Besides representing the sky, it also functions as a sundial, allowing the determination of the sun's longitude and an approximate date given the relationship between the date and the heliocentric longitude. Using the armillary sphere can be seen as a follow-up activity to the manipulation of conventional astrolabes (Egler 2006, Evans 1998), which are two-dimensional projections of the sky onto a plane centered on the observer's position. However, the three-dimensional shape of armillary spheres seems to facilitate the visualization of primitive concepts in positional astronomy and provide an additional resource for understanding astrolabes.

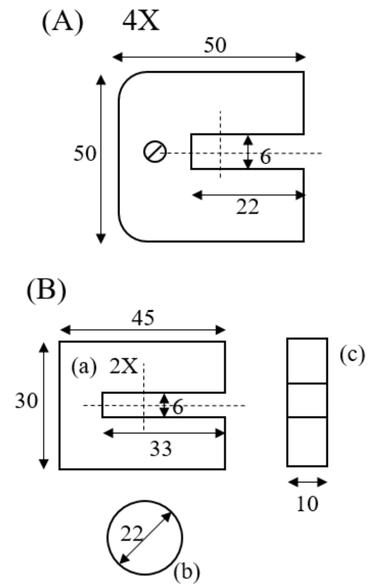

FIG. 12. (A) Drawing of the outer circle clamps Fc used to integrate Cm to Ch. ⊘ is the screw position. (Ba) View of the pole supports Fp used to hold the celestial axis to Cm. (Bb) piece of cork cut as a cylindrical bearing of the south pole. (Bc) fastening strap for the north pole. The finished supports are seen in Fig. 5. All measures are in millimeters.

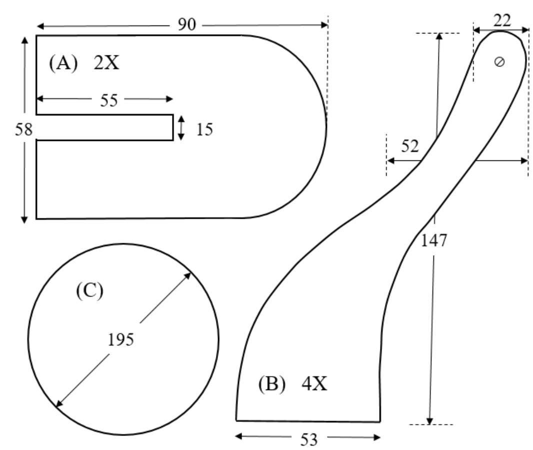

FIG. 13. 2D drawings of the suggested pedestal structure. The pedestal is built as shown in Fig. 3b.

IX. REFERENCES

Alken, P., Chulliat, A., & Nair, M. (2021). NOAA/NCEI and University of Colorado candidate models for IGRF-13. Earth, Planets and Space, 73(1), 1-9.

Aterini, B. (2022). The Armillary Sphere: A Representation of the Celestial Sphere and Knowledge Symbol. In International Symposium on History of Machines and Mechanisms (pp. 330-342). Springer, Cham. https://doi.org/10.1007/978-3-030-98499-1_27

Bennett, J. (2011). Early modern mathematical instruments. Isis, 102(4), 697-705.

Comstock, G. C. (1910). Atmospheric Refraction Near the Horizon. Popular Astronomy, 18, 90-92.

Egler, R. (2006). Measuring the Heavens: Astronomical Instruments before the Telescope. Journal of the Royal Astronomical Society of Canada, 100, 37. https://adsabs.harvard.edu/pdf/2006JRASC.100...37E

Evans, J. (1998). The history and practice of ancient astronomy. Oxford University Press.

Gangui, A., Casazza, R., Paez, C. (2014). From the scale model of the sky to the armillary sphere. The Physics Teacher, 52(7), 403-405. https://doi.org/10.1119/1.4895354

Hughes, D. W., Yallop, B. D., Hohenkerk, C. Y. (1989). The equation of time. Monthly Notices of the Royal Astronomical Society, 238(4), 1529-1535.

Khan, S. (2007). The Armillary Sphere: A Concentrate of Knowledge in Islamic Astronomy. FSTC Limited: Manchester (US).

King, H. C. (2003). The history of the telescope. Courier Corporation.

Lee, Y. S., Kim, S. H., Lee, M. S., Jeong, J. H. (2010). A Study on the Armillary Spheres of the Confucianists in Joseon Dynasty. Journal of Astronomy and Space Sciences, 27(4), 383-392. https://doi.org/10.5140/JASS.2010.27.4.383

Lu, P. (2015). Bhāskara I on the Construction of the Armillary Sphere. History of Science in South Asia, 3, 1-19. https://doi.org/10.18732/H2MW2W

Mosley A. (1999). The Armillary Sphere. Recovered December 28 2022 from http://www.sites.hps.cam.ac.uk/starry/armillary.html

Paselk R. A. (2015). The Armillary Sphere–Maker's Notes. Recovered December 28 2022 from https://www2.humboldt.edu/

Sun, X. (2015). Chinese Armillary Spheres. Handbook of Archaeoastronomy and Ethnoastronomy, 2127.

Wesley, W. G. (1978). The accuracy of Tycho Brahe's instruments. Journal for the History of Astronomy, 9(1), 42-53. https://doi.org/10.1177/002182867800900102

Zhang, J., Sung, Y. T., Hou, H. T., Chang, K. E. (2014). The development and evaluation of an augmented reality-based armillary sphere for astronomical observation instruction. Computers & education, 73, 178-188. https://doi.org/10.1016/j.compedu.2014.01.003

Zotti, G., Hoffmann, S. M., Wolf, A., Chéreau, F., & Chéreau, G. (2021). The simulated sky: Stellarium for cultural astronomy research. arXiv preprint arXiv:2104.01019. https://arxiv.org/ftp/arxiv/papers/2104/2104.01019.pdf